Photonic Function of Materials with Nanometer-Sized Structures

Arao Nakamura, Research Director of CREST
Nagoya University
nakamura@cirse.nagoya-u.ac.jp

1. Introduction

In the research and development of photonic devices with high performance it is of importance to utilize quantum size effects by down sizing of device elements to a nanometer scale. Semimetal/semiconductor heterostructures are expected to facilitate new physics in quantum confined systems and novel electron devices which are potentially important for future high-speed electronics. Nanocomposites consisting of noble metal nanocrystals and glass are also of great interest because of the enhancement in optical and electrical conductance properties that arise from confinement and quantization of conduction electrons in a restricted geometry. In this project, we explore the possibility of control of electronic, magnetic and photonic properties based on quantum size effects with a short optical pulse in two types of heterogeneous materials. We study i) electron transport and magnetic properties in semimetal/semiconductor heterostructures, and ii) ultrafast nonlinear optical properties in metal nanocrystal/insulator composites. We report on several important developments made in this term.

2. Growth of ErP semimetal layers on InP substrates by face-down OMVPE reactor

We installed a newly designed system of organometallinc vapor phase epitaxy (OMVPE) system with a face-down substrate layout. As shown in Fig. 1 the OMVPE system is connected with scanning probe microscopy (SPM) by an ultrahigh vacuum (UHV) tunnel [1]. This system is used to grow rare-earth monopnictides (ErP, CeP, DyP)/semiconductor (InP, GaInP) heterostructures with an atomic level control, and to characterize structures, electronic and magnetic properties. The connected system of OMPVPE and SPM is not common though the system of MBE and SPM is becoming conventional since both are basically UHV facilities. Semimetal ErP layers have been grown on (001)-oriented n^+-InP substrates using TMIn for In, TBP for P, and $(MeCp)_3Er$ for Er as source gases. Surface morphologies and characterization of crystal structures are investigated, and the results are described in [2].

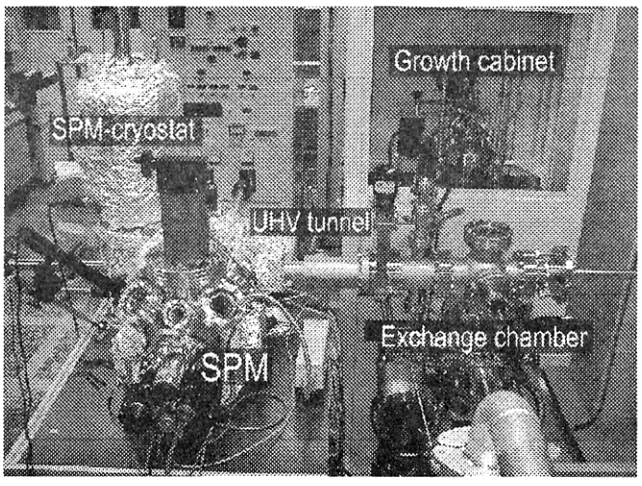

Fig. 1. Completed system of OMVPE growth (right-hand side) and SPM (left-hand side) connected by UHV tunnel (horizontal pipe) and susceptor exchange chamber.

The development of rare-earth sources has been also made. Since the melting point of Er sources ($(MeCp)_3Er$

and $(DPM)_3Er$ which are commercially available is higher than 100 °C, the lines are heated up to 150 °C from source cylinder all through to the nozzles in the OMVPE system. In collaboration with Tri Chemical Lab. Inc. we succeeded to synthesis $(i\text{-}PrCp)_3Er$ and $(EtCp)_3Er$ of which melting points are 57 °C and 62-63 °C, respectively. Thank to the low melting point of these sources the vapor pressure is expected to be higher by a hundred times than that of $(MeCp)_3Er$. We also expect the high growth rate of ErP layers using a new Er source, and the efficiency of heterostructure growth processes will be much improved. $(MeCp)_3Ce$ for a Ce source has been successfully synthesized, which enables us to grow CeP/InP heterostructures.

3. Nanometer scale characterization of electronic properties in single quantum dots

We have studied the morphologies and gap energies of InAs and InGaAs quantum dots (QDs) by using scanning tunneling microscopy/spectroscopy (STM/STS) [3,4]. The results have demonstrated that STM/STS is a powerful technique to investigate both local electronic structure and morphological structure on a nanometer scale. Figure 2(a) shows topographic image of InAs QDs on GaAs(001). The dot height varies from 1.7 to 7.7 nm, and the lateral size is in the range of 14.8 - 32.2 nm. To investigate a correlation between a gap energy and a dot size, the tunneling current was measured with a current imaging tunneling spectroscopy mode. We show in Fig. 2(b) the typical spectra measured for the dots and the wetting layer corresponding to the image shown in Fig. 2(a). The spectrum measured at the wetting layer (area A) yields a gap of 1.5 ± 0.1 eV. The gap energies measured for the QDs with the height of 4.2 (area a) and 5.9 nm (area b) are 1.24 and 0.81 eV, respectively. Comparing the observed height dependence with the calculation based on a quantum disk model, we have found that the gap energy of a single InAs QDs is mainly determined by the quantum confinement in the vertical direction of the QDs. In $In_xGa_{1-x}As$ QDs ($x \sim 0.46$), however, the height dependence of the gap cannot be explained by the quantum confinement model. Taking into account both the confinement and the variation of In composition in a one-dimensional quantum well model, we calculated the gap energy variation with dot height. Comparison of the experiment and calculation has shown that enrichment of In composition takes place in InGaAs QDs [5].

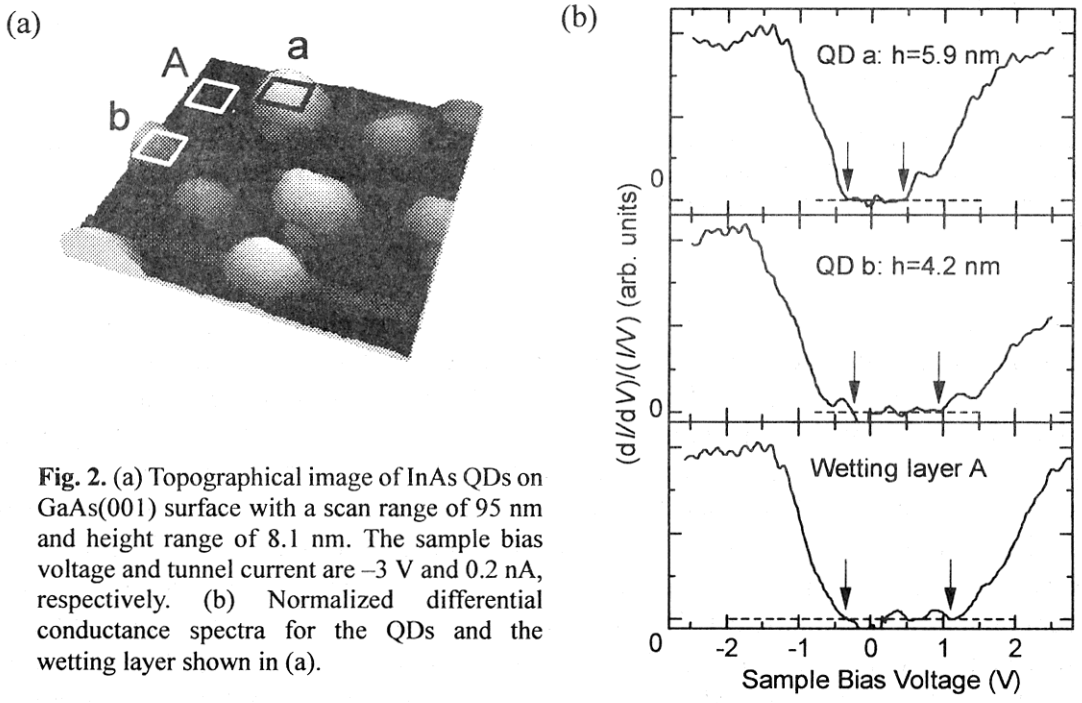

Fig. 2. (a) Topographical image of InAs QDs on GaAs(001) surface with a scan range of 95 nm and height range of 8.1 nm. The sample bias voltage and tunnel current are –3 V and 0.2 nA, respectively. (b) Normalized differential conductance spectra for the QDs and the wetting layer shown in (a).

4. Synthesis and characterization of surface-passivated gold nanoclusters

Using a liquid-phase production method of gold nanoclusters with surface-passivating thiols, we fabricated size-controlled clusters. The structure and size distribution of gold clusters have been investigated by means of transmission electron microscope (TEM), optical absorption measurement and plasma desorption mass spectroscopy (PDMS). From both TEM and PDMS measurements we have found that gold clusters with a diameter of 2 nm are successfully formed [6,7]. Nonlinear optical response of gold nanoclusters has been also studied by femtosecond pump and probe spectroscopy. A preliminary result shows the fast relaxation time of ~1 ps, which suggests the existence of a relaxation channel via breathing modes of nanoclusters [8].

5. Ultrafast response of optical nonlinearity in gold nanocrystal-insulator composites

We have studied a relaxation mechanism that governs a nonlinear response time of a nanocomposite system consisting of nanocrystals and a surrounding material. We have found a new relaxation channel of optically generated hot electrons via breathing vibration damping of nanocrystals in a medium [9]. We prepared gold nanocrystals embedded in three matrix materials, SiO_2, Al_2O_3 and TiO_2 to investigate matrix material- and nanocrystal diameter-dependence of a response time. As shown in Fig. 3 the response time becomes fast with decreasing diameter. The notable result is that the response time shorter for Au/Al_2O_3 than Au/SiO_2. As the bulk modulus of Al_2O_3 is larger than that of SiO_2, this result indicates that the response time is shorter for a matrix with a lager bulk modulus.

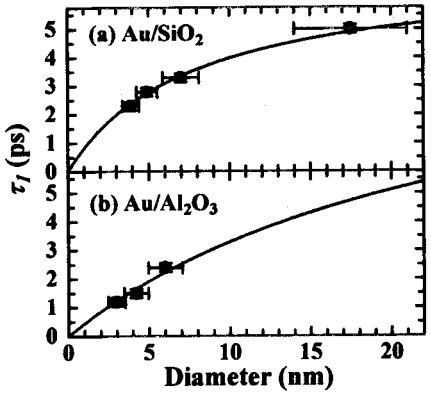

Fig. 3. Diameter dependence of relaxation times for (a) Au/SiO_2 and (b) Au/Al_2O_3. The solid curves show the calculated results.

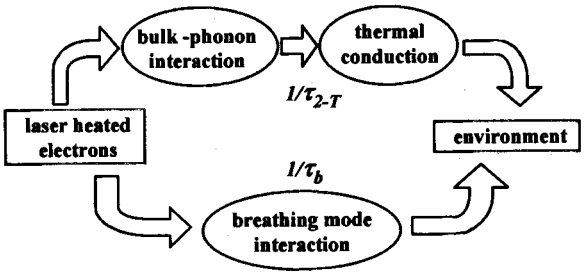

Fig. 4. Schematic diagram of energy relaxation channels of laser heated electrons.

The response time is determined by the decay kinetics of hot electrons created by the optical pulse. Taking account of a breathing vibration of nanocrystals that is characteristic of nanoscale particles, we have analyzed cooling dynamics of hot electrons. Excitation and damping of such a mode have been observed for the present system. The damping time of the breathing mode is proportional to the particle diameter, and depends also on elastic constants of a metal nanocrystal and a matrix. If we take this damping into account as an additional relaxation channel, the total relaxation rate is a sum of the relaxation rate via bulk modes $1/\tau_{2\text{-}T}$ (approximately independent of matrix and diameter) and that via breathing modes $1/\tau_b$ (dependent on matrix and diameter). The calculated results are shown in Fig. 3 by solid curves. The observed dependence of τ_1 on the diameter and matrix can be well reproduced. Compared to the thermal conduction governed by a diffusion constant, the energy transfer via breathing

vibrations is extremely fast, because the oscillation period is on a ps time scale. Such a process is a new class of the electron-energy dissipation process that may be seen in a variety of nano-composite systems with optical and mechanical properties.

6. Electronic states and transport properties of heterostructures including magnetic impurities

A theoretical study has been carried out to investigate electronic states and magnetotransport properties of Mn-doped semiconductors and their resonant tunneling diode (RTD) characteristics [10]. Using a realistic LCAO model and the double exchange type model Hamiltonian we calculated electronic states of (Ga-Mn)As. The results show that there appears a sharp resonant state at the top of the down spin valence band, and the resonant states give rise to a strong and long-range ferromagnetic coupling between Mn moments. This mechanism for the ferromagnetism is thus called as a double resonance mechanism. Spin-dependent conductance has been calculated. The large spin asymmetry of the conductance Γ is obtained to be $\Gamma_{up}/\Gamma_{down} \sim 3$, which suggests that large magnetoresistive effects can be realized in a magnetic junction of (Ga-Mn)As. We have also calculated current-voltage relation of RTD using a model with an effective exchange splitting. The dI/dV-V relation shows a resonant tunneling behavior.

We have also investigated electronic states and resistance of semimetal/semiconductor heterostructures using a simple model [11]. The resistance of the heterojunctions was calculated as a function of energy splitting ΔE between the top of the valence band and the bottom of the conduction band of the semimetal layer. The crossover from semimetal to semiconductor occurs at $\Delta E = 0.2$ taking the hopping integral (0.5 eV) between the nearest neighbor sites as the unit of energy. Luminescence properties of Er-doped semiconductors have been also calculated. The result will be reported in the poster presentation [11].

References

[1] Y. Takeda et al., FEMD Newsletter, Vol. 2, No.4 (2001).
[2] Y. Takeda et al., Symposium Abstracts.
[3] T. Yamauchi et al., Appl. Phys. Lett. 77, (2001) 4368.
[4] T. Yamauchi et al., Appl. Phys. Lett. 77, No. 15 (2001).
[5] T. Yamauchi et al., Symposium Abstracts.
[6] Y. Tai et al., Advanced Materials, (2001) in press.
[7] Y. Tai et al., Symposium Abstracts.
[8] Y. Hamanaka et al., Meetings Abstracts of the Physical Society of Japan, 56, (2001) 659.
[9] Y. Hamanaka et al., Phys. Rev. B63, (2001) 104302.
[10] J. Inoue et al., Phys. Rev. Lett. 85, (2000) 4610.
[11] J. Inoue et al., Symposium Abstracts.

TMIn: trimethylindium, TBP: tertiarybutylphosphine
$(MeCp)_3Er$: trismethylcyclopentadienylerbium
$(DPM)_3Er$: trisdipivaloylmethanatoerbium
$(i\text{-}PrCp)_3Er$: trisisopropylcyclopentadienylerbium
$(EtCp)_3Er$: trismethylcyclopentadienylerbium